Eur J Transl Myol 36 (3) 15606, 2026 doi: 10.4081/ejtm.2026.15606

# In-frame exon skipping induced by the c.14510delA variant in *RYR1*

Daniela Rossi,[1,2] Valentina Guardascione,[1] Matteo Serano,[1] Vincenzo Sorrentino[1,2]

*[1]Department of Molecular and Developmental Medicine, University of Siena, Italy; [2]Program of Molecular Diagnosis of Rare Genetic Diseases, Azienda Ospedaliera Universitaria Senese, Siena, Italy.*

*This article is distributed under the terms of the Creative Commons Attribution Noncommercial License (CC BY-NC 4.0) which permits any noncommercial use, distribution, and reproduction in any medium, provided the original author(s) and source are credited.*

***Abstract***

RNA splicing is a crucial step in eukaryotic gene expression, ensuring the accurate removal of introns and joining of exons to produce mature transcripts. Mutations that alter canonical splice sites or splicing regulatory elements can profoundly affect this process, resulting in aberrant mRNA species and disease. Genetic screening for Malignant Hyperthermia Susceptibility (MHS), resulted in the identification of a frameshift variant in *RYR1* (c.14510delA, rs193922877) associated with MHS and core-like structures in skeletal muscle biopsies. The c.14510delA variant causes a frameshift leading to premature truncation of the protein and loss of the C-terminal transmembrane domains. Splice site prediction analysis suggested that this variant could also impact mRNA splicing. Transcript analysis confirmed that the variant induces in-frame skipping of exon 100, resulting in a shorter *RYR1* transcript where exon 101 follows exon 99. To our knowledge, this represents the first description of an in-frame exon skipping event in *RYR1*. Although the functional impact of the resulting channel isoform remains to be fully elucidated, our findings emphasize the importance of mRNA-level investigations in the molecular diagnosis of *RYR1*-related myopathies.

**Key Words:** alternative splicing, frameshift mutation, transcript analysis, skeletal muscle disorders

*Eur J Transl Myol 36 (3) 15606, 2026 doi: 10.4081/ejtm.2026.15606*

RNA splicing is a fundamental step in eukaryotic gene expression that removes non-coding introns from precursor mRNA and joins exons to generate mature transcripts. This process is catalyzed by the spliceosome, a large ribonucleoprotein complex that recognizes highly conserved sequence motifs at exon–intron junctions: the 5′ splice site (commonly GU), the 3′ splice site (commonly AG), the branch point, and additional surrounding consensus elements.[1] Moreover, Exonic Splicing Enhancers (ESEs) located near splice sites are essential for proper exon recognition, as they recruit Serine/arginine-Rich (SR) proteins that stabilize the binding of spliceosomal components.[2,3]

Alternative splicing, whereby different combinations of exons are joined together, can generate multiple transcript isoforms from a single gene, thereby expanding proteomic diversity. However, mutations in cis-acting splicing regulatory elements or in the canonical splice site motifs can disrupt normal splicing patterns, leading to intron retention, activation of cryptic splice sites, translation re-initiation or exon skipping events. These events may thus cause absence of the corresponding protein due nonsense-mediated mRNA decay, production of truncated proteins due to appearance of pre-mature stop codons or translation re-initiation, or synthesis of functionally altered isoforms with significant pathological consequences.[4] Indeed, such mechanisms have been implicated in several diseases, including Duchenne Muscular Dystrophy (DMD), spinal muscular atrophy, nemaline myopathy, and myotubular myopathy.[5-11] On the other hand, in-frame exon skipping may yield to translation of proteins that are partially functional, whose expression can result in milder disease phenotypes.[1-3] Interestingly, this mechanism has been extensively studied as a potential therapeutic approach to overcome the deleterious effect of non-sense mutations and, nowadays, it represents a currently approved therapy for treatment of DMD.[4]

The *RYR1* gene encodes the ryanodine receptor type 1 channel, responsible for calcium release in skeletal muscle necessary for muscle contraction. Mutations in *RYR1* are associated with alterations in calcium homeostasis that lead to various clinical manifestations including different forms of myopathies that are collectively named as *RYR1*-related myopathies and to Malignant Hyperthermia Susceptibility (MHS), a pharmacogenetic disorder that may lead to uncontrolled increase in body temperature, muscle contraction

and increase in body metabolism in individuals when exposed to muscle relaxant and volatile anesthetics. *RYR1*-related myopathies are characterized by a wide spectrum of clinical phenotype ranging from mild to severe; at the histological level variable phenotypes can be observed, like the presence of central-cores, mini-core, rods, contractures.[12-15] During routine genetic diagnosis of MHS, we identified a novel variant in the *RYR1* gene, c.14510delA (known as rs193922877), associated with malignant hyperthermia and presence of core-like structures in muscle biopsies.[16] Deletion of nucleotide 14510 in exon 100 of the *RYR1* gene results in an alteration of the open reading frame where amino acids Gln4837 and Leu4838 are replaced by Arg and Trp residues, and an opal stop codon appears five nucleotides downstream of the deletion (R4837fsX4839). The mutated RyR1 protein lacks the last 202 amino acid residues in the C-terminal region of the channel, including the putative selectivity filter and the final two transmembrane domains. In addition, splicing site prediction algorithms showed a possible change at donor site 2 bps downstream the nucleotide change. In view of this, we wanted to extend the characterization of the c.14510delA variant, by analyzing the mRNA of family members carrying the variant. We report here evidence that the c.14510delA variant alters mRNA splicing yielding to in-frame skipping of exon 100 and generation of a shorter *RYR1* mRNA where exons 101 follows exon 99. At the best of our knowledge, this is the first case of in-frame exon skipping described in *RYR1,* where out of frame splicing mutations are described;[17-19] we believe that, in the future, considering extending the analysis of *RYR1* variants at the mRNA level may contribute to further characterize the spectrum of *RYR1*-related myopathies.

## Materials and Methods

This study complies with the ethical standards laid down in the 1964 Declaration of Helsinki. The skeletal muscle biopsies from *vastus lateralis* used in this study were collected during routine diagnostic procedures, after obtaining informed consent from all patients.

### *Genomic DNA extraction, PCR and sequencing*

Genomic DNAs were extracted from peripheral blood leucocytes following standard methods[16]. The genomic structure and intron boundary sequences were deduced from the *Homo sapiens* chromosome 19 genomic contig NT_086903.1 and the cDNA sequence NM_000540.1. PCR primers were designed for each exon with the primer-3 software (https://primer3.ut.ee). PCR amplifications were performed in a final volume of 25 µl, containing 100 ng of genomic DNA, 1 X PCR buffer, 0.5 pM of each primer, 180 µM of each dNTP and 1 U of TaqGold DNA polymerase (Thermo Fisher Scientific). The PCR reactions were performed on a MJ research PTC-100 Peltier Thermal Cycler (Global Medical Instrumentation, Minnesota, USA). Amplicons were sequenced by standard Sanger sequencing on an ABI-3100 sequencing apparatus (Applied Biosystems).

### *RNA extraction from skeletal muscle tissue, reverse transcription and PCR amplification*

Total RNA was isolated using the Trizol®Reagent (Thermo Fisher Scientific) following the manufacturer's instructions and quantified by a spectrophotometer at a wavelength of 260 nm (Ultraspec 2100 pro) and stored at -80°C until use.[20] 1 mg of total RNA was retrotranscribed to produce cDNA by using the High-Capacity cDNA Reverse Transcription Kit (Applied Biosystems). The reaction was placed in a thermal cycler (Eppendorf Mastercycler) set on the conditions indicated by the manufacturer. 2 ml of cDNA was used to amplify the regions between nucleotide c.14168 and c.14628 of *RYR1*, containing exons 98 to 101 using the following primers: RyR1-Forward 5'-GCAAGGTCCTGGACAAACAT-3' and RyR1-Reverse 5'-GAGGATGAACCTGACATGAAG-3'. PCR amplifications were performed with Amplitaq Gold Taq Polymerase (Applied Biosystems) following the manufacturer's instructions, using a MJ Research PTC-200 thermal cycler. PCR products were cloned into pGEM T-easy vector following manufacturer's instruction (Promega). Single colonies of the *E.Coli* XL-10 Gold strain transformed with pGEM T-easy recombinant plasmids were selected. Plasmid DNA was isolated and sequenced using appropriate pGEM T-easy specific primers. Sequencing of PCR products was performed by standard capillary Sanger sequencing (Applied Biosystems 3500 Series Genetic Analyzer).

### In vitro *contracture test (IVCT)*

*In Vitro* Contracture Test (IVCT) was performed according to the European Malignant Hyperthermia Guidelines (https://www.emhg.org). Briefly, muscle bundles from *vastus lateralis* were dissected immediately after excision and placed in oxygenated (95% $O_2$, 5% $CO_2$) Krebs-Ringer solution. Bundles were mounted in organ baths at 37°C, attached to a force transducer (Ugo Basile, Italy) and stimulated via field electrodes (1 ms, 0.2 Hz). Separate muscle bundles underwent cumulative drug testing at 3-minute intervals with halothane (Santa Cruz): 0.5, 1.0, 2.0, and 3.0% v/v vaporized into the gas mixture or caffeine (Merk): 0.5, 1.0, 2.0, 3.0, 4.0, and 32.0 mM, added directly to the bath.

According to EMHG guidelines, a sustained baseline tension increase of ≥2 mN (0.2 g) following either halothane or caffeine (or both) was defined as the contracture threshold. Phenotypes were classified as: i) Malignant Hyperthermia Susceptible (MHS): threshold reached at ≤2.0 mM caffeine and ≤2.0% halothane; ii) Malignant Hyperthermia Negative (MHN): no contracture (≥2 mN) at diagnostic concentrations.

### *Histological analyses*

Muscle biopsies from *vastus lateralis* muscle were embedded in Tissue-Tek O.C.T compound (Bio-Optica, Italy), snap frozen in liquid nitrogen-cooled isopentane, and stored at −80°C until further use. Serial 8-µm-thick cryosections were stained with succinate dehydrogenase (SDH) (Bio-Optica, Italy). Sections were examined using

an Axiovert 200 microscope (Zeiss, Germany), and images were acquired at 20x magnification with an Axiocam 702 mono camera (Zeiss, Germany).

### In silico *analysis of the RYR1 c.14510delA variant*

To perform in silico analysis of the RYR1 c.14510delA variant, the SpliceAI software was used. SpliceAI is a copyrighted work by Illumina and is provided under GPLv3 and CC BY NC 4.0 licenses for academic and non-commercial use. It runs the SpliceAI and Pangolin splicing prediction models on user-specified variants and then displays the scores. The following parameters were set up: Genome version hg38; Genecode: basic; Max distance 10000 bp. Prediction: SAI-10k-calc interprets SpliceAI outputs to predict splicing aberration type (pseudoexonization, whole/partial intron retention, partial exon deletion, exon skipping), the size of inserted/deleted sequence, and effect on reading frame. It has 95% sensitivity and 96% specificity, with >81% accuracy for predicting pseudoexon, partial intron retention, and exon skipping.
Other prediction algorithms have been applied by the Alamut Visual Plus version v2.0.1 © 2026 SOPHiA GENETICS.

## Results

### *A variant in the pVSD domain of RYR1 results in premature stop codon and exon skipping*

We previously reported a c.14510delA deletion in exon 100 of the *RYR1* gene, known as rs193922877, in a family where one individual underwent an MHS crisis during surgical procedures under general anesthesia.[16] Genetic anal-

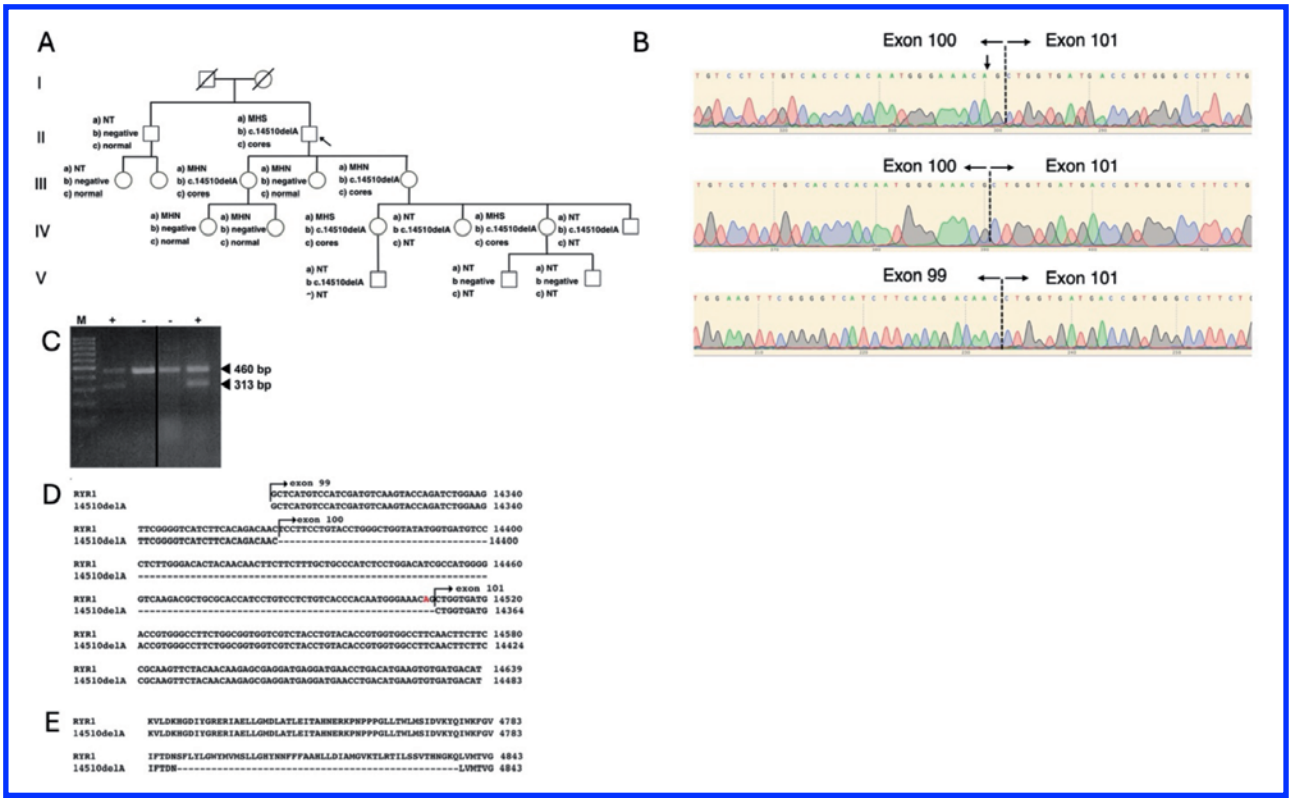


***Figure 1.*** *Analysis of the c.14510delA variant in* RYR1. *A) The family pedigree. The proband is indicated by an arrow. a)* In Vitro *Contracture Test outcome: NT (not tested), MHS (Malignant Hyperthymia Susceptible), MHN (Malignant Hyperthermia Normal); b) Presence (c.14510delA) or absence (negative) of the variant. c) Histological results: central cores (cores), normal, and not investigated (NT). B) Chromatograms of* RYR1 *amplicon sequences. Amplification and sequence analysis of cDNA obtained by RNA extracted by muscle biopsies from normal individuals (upper panel), or carriers of the c.14510delA variant (middle and lower panel) C) Agarose gel electrophoresis of* RYR1 *gene amplicons. RNA from representative individuals carrying (+) or not carrying (-) the c.14510delA variant was extracted, retrotranscribed and amplified using specific primers targeting sequences within exons 98 and 101 of* RYR1. *The black bar indicates the segment where the image was cropped. M=DNA molecular weight marker; arrowheads indicate bands corresponding to fragments of 460 and 313 base pairs. D) Nucleotide sequence alignment of PCR products. cDNA of samples obtained from individuals carrying the* RYR1 *c.14510delA variant and wild type relatives were amplified, cloned into pGEM T-easy vectors and sequenced. The A nucleotide shown in red indicates the nucleotide deleted in the genomic DNA of patients carrying the c.14510delA variant. E) Amino acid sequence alignment between the predicted protein segment encoded by wild type* RYR1 *transcripts (top sequence) and the sequence resulting from exon 100 skipping due to 14510delA variant (bottom sequence).*

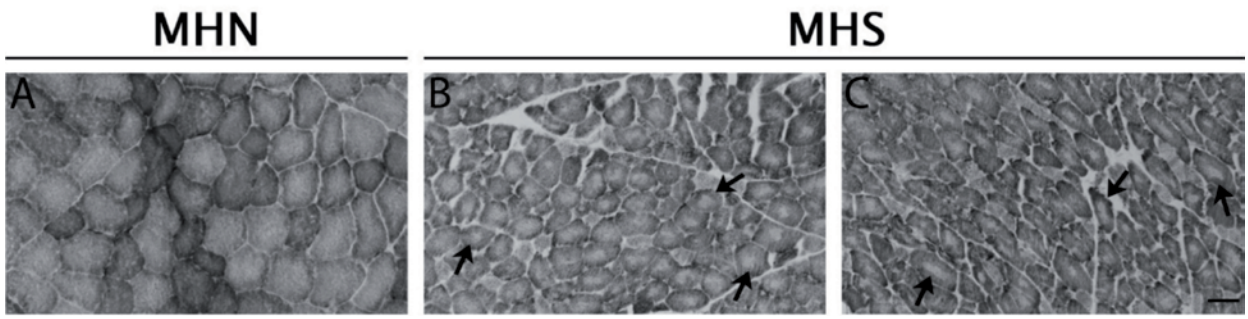


***Figure 2.*** *Histological analysis of the c.14510delA variant in* RYR1. *SDH staining of muscle biopsies from A) MHN (Malignant Hyperthermia Normal) and B-C) MHS (Malignant Hyperthymia Susceptible) patients. Muscle biopsy from patients B and C present several fibers with central cores (indicated by black arrows; SDH-negative areas), whereas patient A shows no evidence of central cores. Scale bar: 50 µm.*

ysis of additional family members revealed that eight individuals carry the c.14510delA variant; five of the c.14510delA carriers underwent an IVCT, but only three resulted susceptible for MHS, indicating a variable penetrance of the variant (Figure 1A). Nevertheless, at the histological analysis, all c.14510delA carriers show the presence of cores depleted of oxidative enzyme staining resembling those observed in patients with core-like myopathy (Figure 1A and Figure 2; Table 1). Since splicing site prediction algorithms showed a possible change at the donor site located 2 bps downstream the nucleotide change (Table 2) we analyzed the mRNA expressed in muscles from four family members carrying the variant and from two healthy relatives (Figure 1A). To this aim, we amplified a region containing exons 98 to 101 of the *RYR1* cDNA. Interestingly, the amplification of the cDNA in subjects carrying the 14510delA variant, resulted in generation of the expected band of 460 bp including sequences from exons 98, 99, 100 and 101 transcribed from either wild type or mutant *RYR1* allele, and of an additional band at lower molecular weight of 313 bp that, after sequence analysis, revealed to correspond to a splice variant, where exon 100 was skipped to generate a shorter RYR1 mRNA where exons 101 follows exon 99 (Figure 1B-D). This splicing allows to maintain the open reading frame of the *RYR1* transcript, potentially generating a RyR1 channel lacking 49 amino acids in the pVSD domain and, in particular, in the S3 segment of the trans-

***Table 1.*** *Family summary table of the relationship among genotype, IVCT results, histological abnormalities, and clinical phenotype. Subject ID is relative to the family pedigree in Fig 1A; IVCT (*In Vitro *Contracture Test).*

| Subject | Genotype | IVCT diagnosis | Age at biopsy | Histological findings | Clinical Phenotype |
|---|---|---|---|---|---|
| II2 | c.14510delA | MHS | 77 | Central Cores; Prevalence of type I fibers | Mild muscle weakness; no increase in CPK |
| III3 | c.14510delA | MHN | 53 | Central Cores; Prevalence of type I fibers | Asymptomatic |
| III4 | Negative | MHN | Data not available | Not tested | Asymptomatic |
| III5 | c.14510delA | MHN | Data not available | Central Cores; Prevalence of type I fibers | Asymptomatic |
| IV3 | c.14510delA | MHS | 39 | Central Cores; Prevalence of type I fibers | Asymptomatic |
| IV5 | c.14510delA | MHS | 38 | Central Cores; Prevalence of type I fibers | Asymptomatic |

***Table 2.*** *Summary of splicing prediction analysis according to Alamut Visual Plus version v2.0.1.*

| Donor Sites | SSF [0-100] | MaxEnt [0-12] | NNSPLICE [0-1] | GeneSplicer [0-24] | SPiP [0-1] |
|---|---|---|---|---|---|
| Threshold | ≥70 | ≥0 | ≥0.4 | ≥0 | No threshold |
| **Exon 100 -c.14511 N** | **80.45 ⇒ 71.22 (-11.5%)** | **6.34 ⇒ 4.66 (-26.5%)** | **0.84 ⇒ —** | **8.26 ⇒ 3.93 (-52.4%)** | **0.0698 ⇒ 0.0233 (-66.6%)** |

*N, Natural Splice Site.*
*Splicing Pipeline Prediction (SPiP): Overall prediction: The mutation alters the consensus splice sites. Risk that the variant impacts splicing: 100% [97.32% - 100%]. SPiP score: 0.852. SPiCE class (high/medium/low): high. SPiCE probability for variant in consensus splice site: 0.90054. Nearest natural splice site to the variant: donor. Relative distance between the nearest splice site and the mutation: -2. Type of region where the variant is located: Exonic Splicing Regulator Consensus. Relative distance between the cryptic site and the natural site: -2. SSF, Splice Site Finder; MaxEntScan, Maximum Entropy Scan; NNSplice, Neural Network Splice site predictor NNSPLICE 0.9 (Berkeley Drosophila Genome Project).*

membrane domain (Figure 1E).[21-23] A relative quantification of the expression levels of the *RYR1* transcripts performed in two out of four individuals showed that, in the first individual, 62.86% of the *RYR1* transcripts corresponded to those transcribed by the wild type allele, 31.43% of the transcripts corresponded to those transcribed by the mutant allele and 5.7% of the transcripts were generated by skipping of exon 100. In the second individual, the percentage of transcripts where exon 100 was skipped was 12.9% (54.84% of the transcripts were transcribed by the wild type allele and 32.26% of the transcripts were transcribed by the mutant allele). mRNA corresponding to skipping of exon 100 were not observed in mRNAs extracted from 21 control individuals and 12 MHS individuals carrying other *RYR1* variants (not shown).

### *Histological analysis of muscle biopsies from individuals carrying the c.14510delA deletion reveal the presence of core-like lesions*

We previously reported that histological analysis of muscle biopsy from individuals carrying the c.14510delA variant in *RYR1* revealed the presence of 80% of fibers showing cores-like lesion and a prevalence of type 1 fibers.[16] To extend our analysis we performed histological analysis on additional family members and found that all available biopsies from individuals carrying the 14510delA *RYR1* variant show core-like lesions and prevalence of type I fibers, suggesting that these may be reasonably considered as typical traits of the myopathy associated to this variant (Figure 2).

## Discussion

Exon-skipping mutations represent a class of genetic alterations that can have major implications in both the diagnosis and the pathogenesis of genetic diseases.[4] These mutations may arise from changes at canonical splice sites, in splicing regulatory elements or within introns that result in creation of cryptic splice sites. When an exon is skipped, the reading frame may be maintained ("in-frame skip") or disrupted ("out-of-frame skip"), and this determines whether the resultant protein is truncated, degraded, or whether a partially functional protein is produced. In this last case, exon skipping can lead to a phenotype that is milder than expected. A well-known example is provided by point mutations in the DMD gene that promote exon skipping in vivo, resulting in residual dystrophin expression and a shift from a severe Duchenne to a milder Becker phenotype.[24]

From a diagnostic point of view, exon skipping introduces considerable complexity in establishing genotype–phenotype correlations and predicting disease severity. Moreover, exon-skipping mutations are often under-recognized when only DNA-based testing is performed. Thus transcript-based assays are increasingly important to verify whether a variant causes aberrant splicing or skipping. Failure to detect or interpret exon-skipping events may lead to misclassification of pathogenicity, incorrect prognosis, or suboptimal genetic counseling.

We report here on the identification of a variant that induces an exon-skipping in *RYR1,* c.14510delA, in eight members of a family, three of which tested positive at the IVCT while all carriers displayed core-like lesions in muscle biopsies. This variant promotes the skipping of exon 100, producing a transcript that encodes a RyR1 subunit lacking 49 amino acids in the pVSD domain. The c.14510delA variant is located two nucleotides upstream the end of exon 100, a region that is considered critical for the recognition of the donor splicing site by the spliceosome U1 snRNP component. SpliceAI predicts a strong splice-disruptive effect for this variant, with an overall splice loss $\Delta = 0.57$ and donor loss $\Delta = 0.38$ at +2 bp, accompanied by a modest donor gain $\Delta = 0.21$ ap-

proximately 109 bp downstream. These scores suggest that the variant may weaken the canonical donor site and promote usage of a cryptic downstream donor site, potentially resulting in partial exon skipping or aberrant splicing.[25] Consistently, MaxEntScan analysis shows a decrease in the canonical donor site strength from 6.34 to 4.66, corresponding to an approximate 26.5% reduction in predicted splice-site strength.[26] Such a decrease indicates a moderate weakening of the donor site, supporting the SpliceAI prediction of reduced donor recognition efficiency.

Exon-skipped transcripts are expressed at lower levels than the wild-type mRNA, with approximately 50–60% of transcripts being wild-type, 30% carrying the c.14510delA variant, and no more than 12.9% lacking exon 100. Alternatively, the transcripts generated by skipping of exon 100 may be degraded at a higher rate than wild type or mutant mRNAs. Previous studies have shown that in HEK293 cells expressing recombinant *RYR1* c.14510delA cDNA, the corresponding mRNA is not substantially degraded by nonsense-mediated decay and can be translated into a truncated protein that is expressed at levels comparable to wild-type;[16] although we have no direct experimental data, it may be reasonable to think that this may also occur for the mRNA containing the skipped exons in skeletal muscle of c.14510delA carriers. Biochemical analyses indicate that heteromeric RyR1 channels composed of wild-type and truncated subunits exhibit reduced stability and impaired assembly within the tetramer.[16] The presence of core-like lesions in 100% of the carriers suggests that the c.14510delA variant has full penetrance regarding structural muscle remodeling. Conversely, the incomplete penetrance for MHS (3 out of 5 tested) suggests that the hypermetabolic reaction during the IVCT/anesthesia requires additional, yet unidentified factors, that govern calcium release kinetics under stress. Notably, however, the clinical phenotype of c.14510delA carriers is significantly milder than expected, with absent signs of myopathy, suggesting partial preservation of RyR1 channel function.

Interestingly, the identification of a third transcript generated by exon 100 skipping may help to explain this attenuated phenotype. Assuming random tetramer assembly of available RyR1 subunits, combinatorial modeling predicts that the presence of a third subunit type (lacking 49 amino acids) roughly doubles the fraction of RyR1 channels composed by 4 wild-type subunits, compared to a model containing only wild-type and truncated subunits. Specifically, the probabilities of channels containing 0, 1, 2, 3, or 4 wild-type subunits change from 6.25%, 25.00%, 37.50%, 25.00%, and 6.25% to 2.56%, 15.36%, 34.56%, 34.56%, and 12.96%, respectively. These results indicate that, even if modest, the increase in the fraction of functional subunits can partially mitigate the dominant-negative effect of the premature stop codon, when assembly occurs stochastically.

In conclusion, mutations that cause exon-skipping are emerging as important mechanism in the pathogenesis of muscle diseases, influencing both molecular and clinical outcomes. Recognition of their role not only improves our understanding of disease variability but also highlights the need for integrated genomic and transcriptomic analyses to achieve accurate diagnosis and refined genotype–phenotype correlations.

## List of abbreviations

MHS, Malignant Hyperthermia Susceptibility
ESEs, Exonic Splicing Enhancers
DMD, Duchenne Muscular Dystrophy

## Funding

Center for Gene Therapy and Drugs Based on RNA Technology, funded in the framework of the National Recovery and Resilience Plan (NRRP), M4C2 Inv, 1.4 CUP B63C22000610006 - Spoke 1" and from the Tuscan Health Ecosystem, funded in the framework of the National Recovery and Resilience Plan (NRRP), Missione 4 Componente 2 Inv. 1.5 CUP B63C22000680007 - Spoke 7". Both grants are, in turn, funded by the European Union-Next Generation EU.

## Contributions

Daniela Rossi, conceptualization, investigation, methodology, writing original draft, funding acquisition; Valentina Guardascione, methodology; Matteo Serano, investigation, methodology; Vincenzo Sorrentino, conceptualization, funding acquisition, writing review and editing.

## Conflicts of interests

This work was supported by funding dedicated to research on genetic myopathies to Vincenzo Sorrentino (see Funding); the author declares no potential conflicts of interest

## Ethics approval

The Ethics Committee of the Tuscany Region approved this study (Protocol No. 16342). The study is conformed with the Helsinki Declaration of 1964, as revised in 2013, concerning human and animal rights.

## Informed consent

All patients participating in this study signed a written informed consent form for participating in this study.

## Patient consent for publication

Written informed consent was obtained from a legally authorized representative(s) for anonymized patient information to be published in this article.

## Availability of data and materials

All data generated or analyzed during this study are included in this published article.

## Corresponding author

Daniela Rossi, Department of Molecular and Developmental Medicine – University of Siena, Via Aldo Moro, 2 53100 Siena (Italy).
Tel.: +39 0577 232903
E-mail: daniela.rossi@unisi.it
ORCID ID: 0000-0003-0463-7327.

## Co-authors

*Valentina Guardascione*
*E-mail: valentina.guardas@student.unisi.it*
*ORCID ID: 0009-0007-1268-1965*

*Matteo Serano*
*E-mail: matteo.serano@unisi.it*
*ORCID ID: 0000-0002-4151-2980*

*Vincenzo Sorrentino*
*E-mail: vincenzo.sorrentino@unisi.it*
*ORCID ID: 0000-0002-8573-8631*

## References

Wahl MC, Will CL, Lührmann R. The spliceosome: design principles of a dynamic RNP machine. Cell 2009;136:701–18.
Blencowe BJ. Exonic splicing enhancers: mechanism of action, diversity and role in human genetic diseases. Trends Biochem Sci 2000;25:106–10.
Jobbins AM, Reichenbach LF, Lucas CM, et al. The mechanisms of a mammalian splicing enhancer. Nucleic Acids Res 2018;46:2145–58.
Scotti MM, Swanson MS. RNA mis-splicing in disease. Nat Rev Genet 2016;17:19–32.
Chu CS, Trapnell BC, Curristin S, et al. Genetic basis of variable exon 9 skipping in cystic fibrosis transmembrane conductance regulator mRNA. Nat Genet 1993;3:151–6.
Muchir A, Bonne G, van der Kooi AJ, et al. Identification of mutations in the gene encoding lamins A/C in autosomal dominant limb girdle muscular dystrophy with atrioventricular conduction disturbances (LGMD1B). Hum Mol Genet 2000;9:1453–9.
Vasli N, Laugel V, Böhm J, et al. Myotubular myopathy caused by multiple abnormal splicing variants in the MTM1 RNA in a patient with a mild phenotype. Eur J Hum Genet 2012;20:701–4.
Torella A, Zanobio M, Zeuli R, et al. The position of nonsense mutations can predict the phenotype severity: A survey on the DMD gene. PLoS One 2020;15: e0237803.
Flucher BE. Skeletal muscle CaV1.1 channelopathies. Pflugers Arch 2020;472:739–54.
Singh NN, O'Leary CA, Eich T, et al. Structural Context of a Critical Exon of Spinal Muscular Atrophy Gene. Front Mol Biosci 2022;9:928581.
Merlini L, Sabatelli P, Cenni V, et al. Myopathic Ehlers-Danlos Syndrome (mEDS) Related to COL12A1: Two Novel Families and Literature Review. Int J Mol Sci 2025;26:5387.
Todd JJ, Sagar V, Lawal TA, et al. Correlation of phenotype with genotype and protein structure in RYR1-related disorders. J Neurol 2018;265:2506–24.
Rossi D, Catallo MR, Pierantozzi E, Sorrentino V. Mutations in proteins involved in E-C coupling and SOCE and congenital myopathies. J Gen Physiol 2022;154: e202213115.
Rossi D, Pranzo C, Roccabianca S, et al. Identification of novel potentially causative RYR1 variants in individuals with malignant hyperthermia susceptibility. Neuromuscul Disord 2026;58:106296.
Ogasawara M, Nishino I. Update on RYR1-related myopathies. Curr Opin Neurol 2024;37:504–8.
Rossi D, De Smet P, Lyfenko A, et al. A truncation in the RYR1 gene associated with central core lesions in skeletal muscle fibres. J Med Genet 2007;44:e67.
Monnier N, Ferreiro A, Marty I, et al. A homozygous splicing mutation causing a depletion of skeletal muscle RYR1 is associated with multi-minicore disease congenital myopathy with ophthalmoplegia. Hum Mol Genet 2003;12:1171–78.
Zullo A, Perrotta G, D'Angelo R, et al. RYR1 Sequence variants in myopathies: expression and functional studies in two families. Biomed Res Int 2019;7638946.
Zhao Q, Li X, Liu L, et al. Prenatal diagnosis identifies compound heterozygous variants in RYR1 that causes ultrasound abnormalities in a fetus. BMC Med Genomics 2022;15:202.
Pierantozzi E, Badin M, Vezzani B, et al. Human pericytes isolated from adipose tissue have better differentiation abilities than their mesenchymal stem cell counterparts. Cell Tissue Res 2015;361:769–78.
des Georges A, Clarke OB, Zalk R, et al. Structural basis for gating and activation of RyR1. Cell 2016;167:145-57.e17.
Samsó M. A guide to the 3D structure of the ryanodine receptor type 1 by cryoEM. Protein Sci 2017;26:52–68.
Woll KA, Van Petegem F. Calcium-release channels: structure and function of IP3 receptors and ryanodine receptors. Physiol Rev 2022;102:209–68.
Okubo M, Noguchi S, Hayashi S, et al. Exon skipping induced by nonsense/frameshift mutations in DMD gene results in Becker muscular dystrophy. Hum Genet 2020;139:247–55.
Jaganathan K, Kyriazopoulou Panagiotopoulou S, McRae JF, et al. Predicting Splicing from Primary Sequence with Deep Learning. Cell 2019; 176:535-48.e24.
Yeo G, Burge CB. Maximum entropy modeling of short sequence motifs with applications to RNA splicing signals. J Comput Biol 2004;11:377–94.

## Disclaimer

All claims expressed in this article are solely those of the authors and do not necessarily represent those of their affiliated organizations, or those of the publisher, the editors and the reviewers. Any product that may be evaluated in this article or claim that may be made by its manufacturer is not guaranteed or endorsed by the publisher.

Submitted: 29 April 2026.
Accepted: 2 June 2026.
Early access: 26 August 2026.